ACS APPLIED MATERIALS & INTERFACES

Research Article

www.acsami.org

Bioinspired Omnidirectional Self-Stable Reflectors with Multiscale Hierarchical Structures

Zhiwu Han,[†,∥] Zhengzhi Mu,[†,‡,§,∥] Bo Li,[†] Xiaoming Feng,[†] Ze Wang,[†] Junqiu Zhang,[†] Shichao Niu,*[,†] and Luquan Ren[†]

[†]Key Laboratory of Bionic Engineering, Ministry of Education, Jilin University, Changchun 130022, China

[‡]Department of Chemical Engineering and [§]Biointerfaces Institute, University of Michigan, Ann Arbor, Michigan 48109-2136, United States

Supporting Information

ABSTRACT: Structured surfaces, demonstrating various wondrous physicochemical performances, are ubiquitous phenomena in nature. Butterfly wings with impressive structural colors are an interesting example for multiscale hierarchical structures (MHSs). However, most natural structural colors are relatively unstable and highly sensitive to incident angles, which limit their potential practical applications to a certain extent. Here, we reported a bioinspired color reflector with omnidirectional reflective self-stable (ORS) properties, which is inspired by the wing scales of *Papilio palinurus* butterfly. Through experimental exploration and theoretical analysis, it was found that the vivid colors of such butterfly wings are structure-based and possess novel ORS properties, which attributes to the multiple optical actions between light and the complex structures coupling the inverse opal-like structures (IOSs) and stacked lamellar ridges (SLRs). On the basis of this, we designed and successfully fabricated the SiO_2-based bioinspired color reflectors (BCRs) through a facile and effective biotemplate method. It was confirmed that the MHSs in biotemplate are inherited by the obtained SiO_2-based BCRs. More importantly, the SiO_2-based BCRs also demonstrated the similar ORS properties in a wide wavelength range. We forcefully anticipate that the reported MHS-based ORS performance discovered in butterfly wing scales here could offer new thoughts for scientists to solve unstable reflection issues in particular optical field. The involved biotemplate fabrication method offers a facile and effective strategy for fabricating functional nanomaterials or bioinspired nanodevices with 3D complex nanostructures, such as structured optical devices, displays, and optoelectronic equipment.

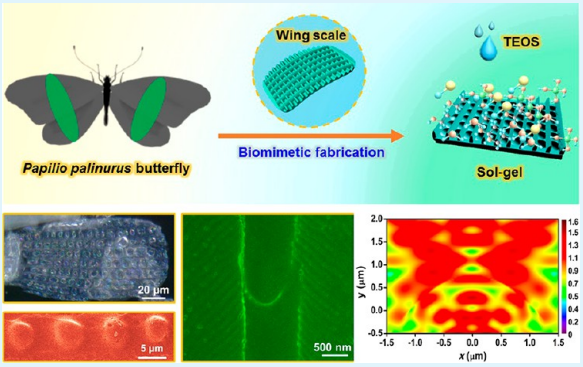

KEYWORDS: *butterfly wing scales, hierarchical structures, optical stability, biomimetic fabrication, bioinspired reflectors*

INTRODUCTION

Structured surfaces are very common in nature and usually exhibit excellent physicochemical properties, such as structural colors of butterfly wings,[1−5] water transport of *Nepenthes alata*,[6] antireflectivity of moth eyes,[7,8] self-cleaning of lotus leaf,[9] fog collection of cactus,[10,11] and water repellent of water striders.[12] Among all these natural structured surfaces, perhaps butterfly wings with multiscale hierarchical structures (MHSs) are the most famous due to their impressive structural colors. In fact, the MHS-based structural colors play critical roles in many butterfly behaviors, such as courtship display, camouflage, and aposematic coloration. So, it has also attracted increasing interests in a wide variety of research fields including biology, genetics, photonics, and material science.[2,13−19] In previous research, one of the properties most mentioned of structural colors is angular dependence.[2,20] Namely, most structural colors are sensitive to incident angles. However, unstable structural colors not only make a big challenge for accurate color characterizations but also greatly limit the potential practical applications.

In general, high-quality structural colors are mostly determined by graceful micro/nanostructures and their ingenious orderly arrangements.[13] Although many scientists and engineers have devoted themselves to design and develop structured surfaces with structural colors for desirable application, such as display, cloaking, and apparel, most methods employed to fabricate structured surfaces are programming complexity, time-consuming and costly with large and expensive equipment, such as atomic layer deposition (ALD),[21−23] electron-beam lithography (EBL),[24] nanoimprint lithography (NIL),[23,25] holographic lithography,[26] template method,[27−29] physical vapor deposition (PVD),[30] layer-by-layer (LBL) deposition,[31] focused ion beam-assisted chemical vapor

Received: June 18, 2017
Accepted: August 3, 2017
Published: August 3, 2017

DOI: 10.1021/acsami.7b08768
ACS Appl. Mater. Interfaces 2017, 9, 29285−29294

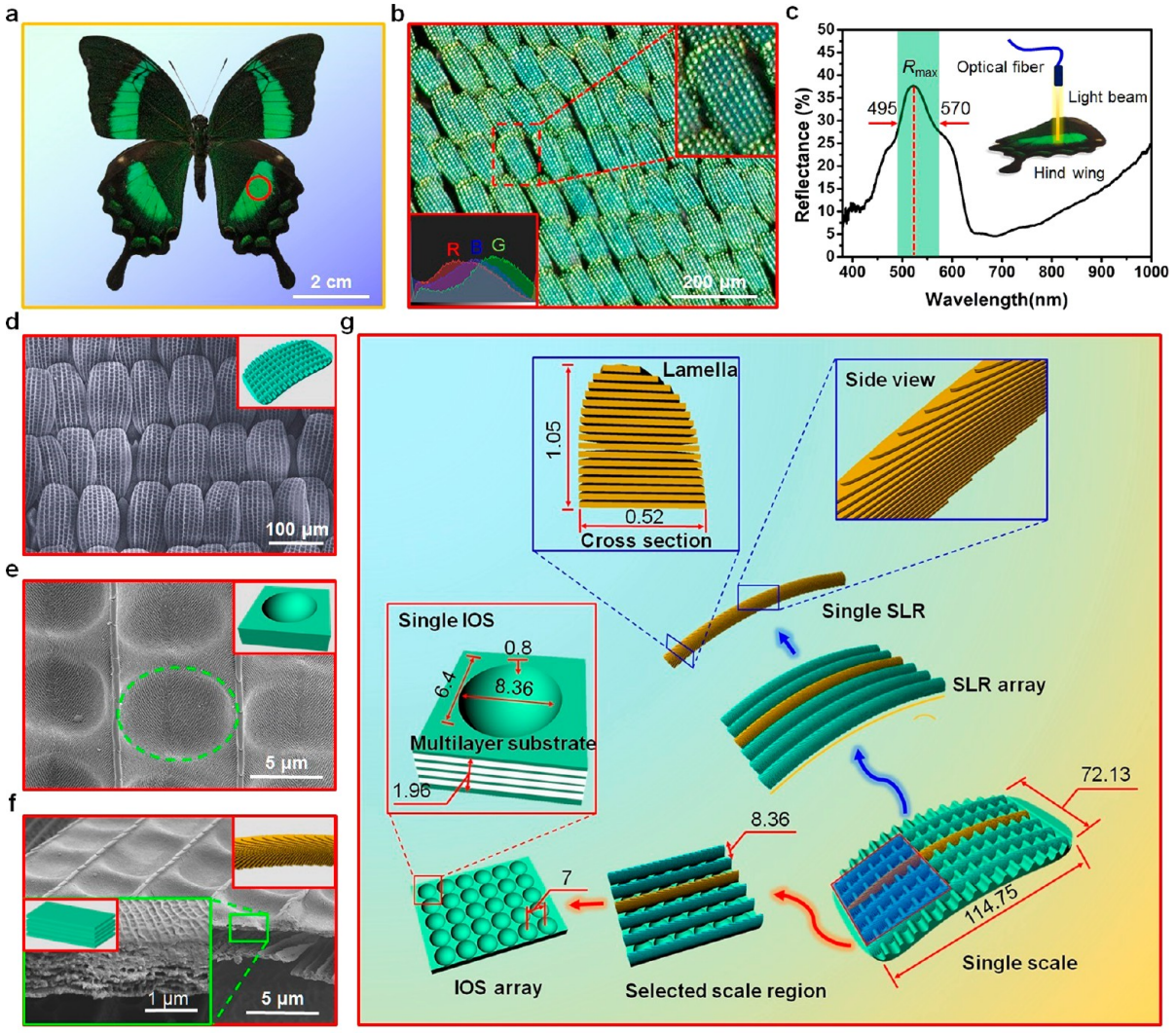

Figure 1. (a) Intact male *Papilio palinurus* butterfly exhibiting brilliant axisymmetric green scale regions. (b) 3D ultradepth stereoscopic microscope image of the green scale region and its RGB distribution. (c) Reflective spectrum of the green scale region at normal incidence. (d) Scale array composed of multitudinous leaflike scales (inset) arranging in order. (e) Oval IOSs (inset) and narrow SLRs constituting the primary structures in a single scale. (f) Cross-section of the single scale showing the parallel SLRs (inset) and IOSs with multilayer (inset). (g) Schematic illustration of structural models showing different feature structures of the single scale: oval IOS, multilayer substrate, and narrow SLR. Measurement unit: μm.

deposition (FIB-CVD),[31,32] and reactive ion etching (RIE).[24,26,33−37] In addition, most conventional artificial structures are relatively simple and usually lack of inspiration.[38] Fortunately, through the course of adaptive evolution and natural selection, the optimal MHSs of butterfly wings have diversified and enriched the sources of inspiration for scientists and engineers. In the past decades, variable bioinspired materials with structural colors have been developed all over the world.[38−42] Particularly, biomimetic fabrication of the MHSs in butterfly wing scales has attracted broad attention and becomes a research hotspot.[43−46] Although a few attempts have been made to fabricate such MHSs,[47−49] there is still space to explore further for these intricate structures with structural colors.

Here, we reported the MHS-based omnidirectional reflective self-stable (ORS) properties of *Papilio palinurus* butterfly wing scales. These structural colors are firmly stable to incident angles in a wide angle range. The ORS properties allow the butterfly wings to keep omnidirectional vivid green colors. Meanwhile, the underlying formation mechanism of the ORS properties was deeply investigated experimentally and theoretically. Moreover, we designed and fabricated the SiO_2-based bioinspired color reflectors (BCRs) in a relative large scale (ca. 1 cm^2) using a highly effective biotemplate method at very low cost. The BCRs are as insensitive to angle as original wing scales and demonstrate similar structural colors over a wide angle range. This work extends the optical performance of natural structural colors to some degree. It can also possibly bridge the gap between pure fundamental theories and potential practical applications of natural complex structures in photodetectors, displays, micromachining, biosensors, etc.

RESULTS AND DISCUSSION

MHSs in Original Wing Scales. *Papilio palinurus* butterflies, a rare large swallowtail butterfly belonging to the family *Papilionidae*,[20] spread in tropical rainforests all over the world. There are distinctive biological features can be found to identify this butterfly. In this case, the wingspan of a male individual is approximately 6.6 cm (Figure 1a). Crescent green scale regions are orderly distributed on both fore and hind

DOI: 10.1021/acsami.7b08768
ACS Appl. Mater. Interfaces 2017, 9, 29285−29294

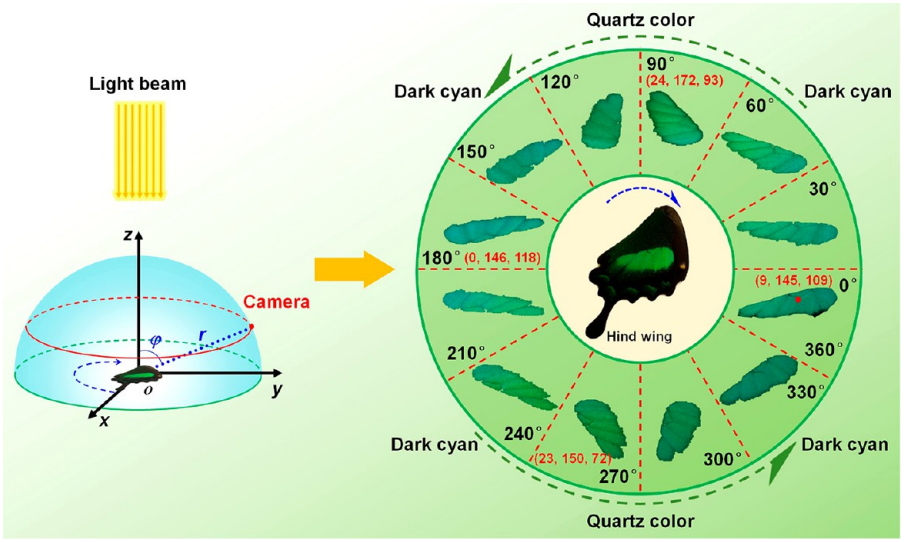

Figure 2. Miniature camera was set at a fixed site (r, φ, 90°) in an observation hemisphere system. Here, r is radius of the sphere, φ is the angle between the segment and the z-axis, and 90° represents azimuths. Parallel light beam illuminates the selected scale region at normal incidence (left). The hind wing in the inner circle rotated along the clockwise at interval of 30°, and the corresponding external separated sectors demonstrated the color variations of the hind wing at the same interval within 360° (right).

wings. Obviously, shiny rectangle patches presenting vivid green color between two adjacent nervures can be easily identified. With the help of 3D ultradepth stereoscopic microscope, biological morphologies and mix-colors (RGB, a general color model) of the original wing scales are characterized (Figure 1b). It is clear that the oval wing scales are arranged in good order on the wing surface along the veins, resembling tiles on a roof. All these scales are the similar shapes and sizes. A single scale is approximately 122 μm long and 61 μm wide. Interestingly, every scale is found riddled with numerous shiny tiny points. These points are distributed all over the scale surface along the length. All these microscale twinkling wing scale arrays work together to make the whole butterfly wings vivid on a macro-scale, which can be observed directly by naked eyes. To quantize the optical performance properties of the original wing scales, the reflective properties of the green scale regions are characterized using a miniature fiber-optic spectrometer. As expected, a strong feature peak ($R_{max} \approx$ 38.5%) appears at 526 nm, which is consistent with the green color waveband (495−570 nm) (Figure 1c).

To reveal the underlying structural basis of the natural structural colors, surface topographies of a single scale are characterized using ultrahigh-resolution field emission scanning electron microscope (FESEM). Interestingly, dense inverse opal-like pits are distributed all over the scale surface (Figure 1d). The density of these pits is approximately 140 per scale. To some degree, the areas of these pits seem to conform to Gaussian distribution (Figure S1). It is noted that these scales are spontaneously arranged in alternate rows and overlap with each other. There are about 9 ridges along the length in every single scale. These periodic ridge structures are also confirmed by X-ray diffraction (XRD) spectrum (Figure S2). The rim of the pits resembles an oval (Figure 1e). All these pits are located between two adjacent ridges. Besides, fine secondary structures of the pits and the ridges are also investigated in detail. The bottoms and jambs of the pits are covered by closely aligned grids. To obtain the 3D morphology of the single scale, the specimen is crosscut along the width of the scale using a lancet. The cross section of the apocoptic scale presents the ridges composed of overlapped narrow lamellae, which are exactly tangent to the oval. It also indicates the concave composed of multiple layers is about 1 μm. In addition, there is a thin air layer between adjacent layers (Figure 1f).

According to the aforementioned FESEM results, 3D visual structural models are built to clearly illustrate the MHSs of the original wing scale (Figure 1g). The whole single scale bends slightly to form an arc. It is about 114.75 μm long and 72.13 μm wide. The secondary structures are pulled off seriatim. On one hand, the single ridge is selected from the bent ridge array. The side view of the single ridge shows overlapped lamellae resembling shutters. The multilayer system is composed of the alternate lamella layers and air layers as shown in the cross section. On the other hand, a complanate region is split up to illustrate the specific dimensions of the feature structures. The inverse opal-like structure (IOS) array is fully revealed when stacked lamellar ridge (SLR) array is completely removed. The spacing between two adjacent ridges is about 8.36 μm. The center distance between two adjacent IOSs is measured along the length. It is about 7.00 μm. In order to roundly quantize the IOS array, single IOS is amplified and its 3D structural feature sizes are indicated. The long axis and short axis of the ellipse are 8.36 and 6.40 μm, respectively. The depth of the single IOS is about 800 nm. In addition, the thickness of the multilayer substrate is about 2.03 μm. It is clear that the structure system of the single scale is composed of simple primary structures and fine secondary structures on the wavy scale base surface (Figure S3). It suggests that the dimensions of these structures involve three different orders of magnitude: millimeter (mm), micrometer (μm) and nanometer (nm). Thus, the fundamental structure system of original wing scales is not only hierarchical but also multiscale.

Dynamic Characterizations of the MHS-Based Structural Colors. In general, visual colors can be divided into two color types: structural colors (physical color) and pigment (chemical color). In this case, to confirm the color type of the green scale regions, we carried out a simple discoloration experiment using ethyl alcohol (EtOH, A. R.) (Movie S1). First, the vivid green scale regions gradually become dim. Then,

DOI: 10.1021/acsami.7b08768
ACS Appl. Mater. Interfaces 2017, 9, 29285−29294

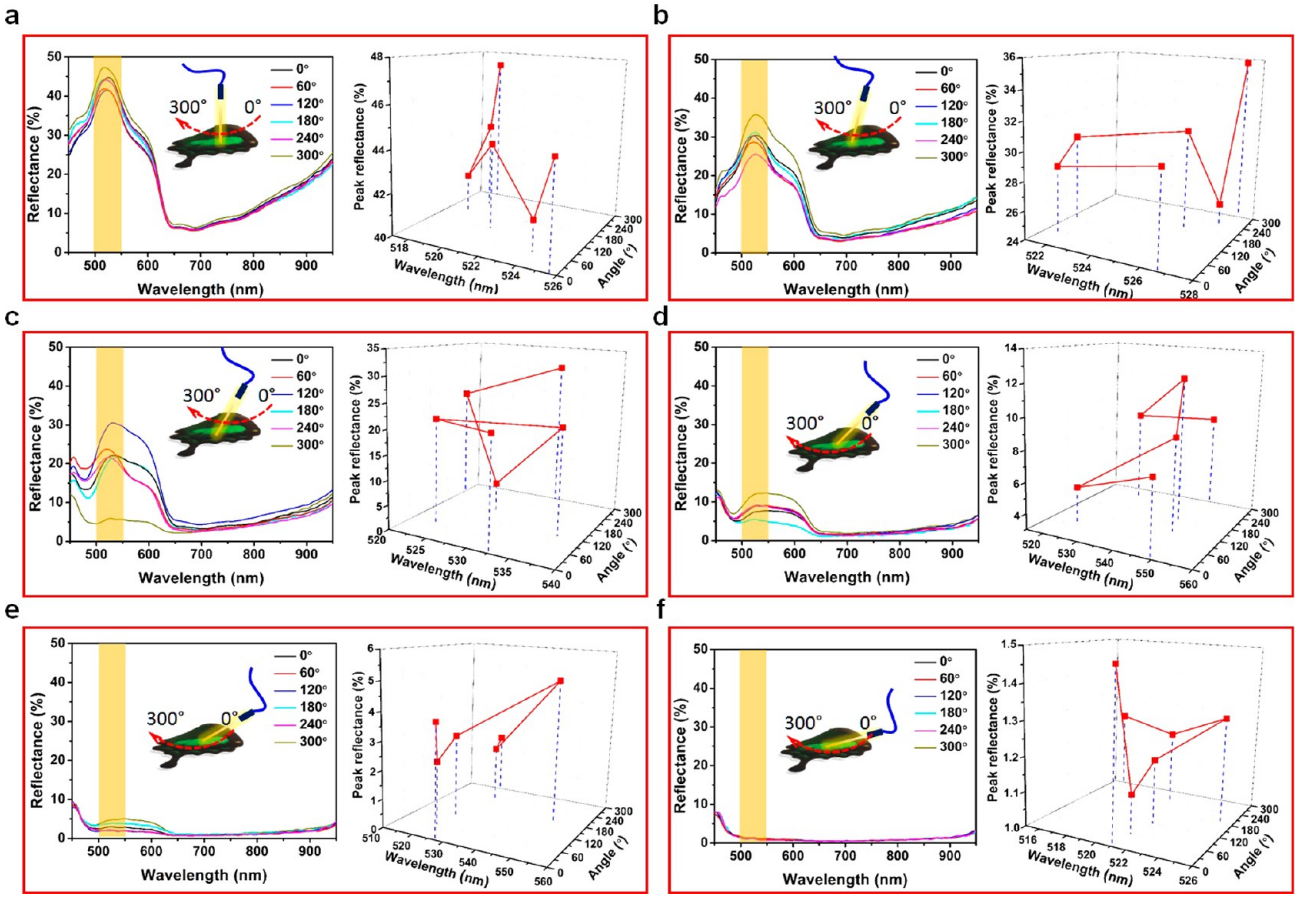

Figure 3. Experimental reflectance spectra of the ORS properties with variable angles at different incident angles: (a) 0, (b) 15, (c) 30, (d) 45, (e) 60, and (f) 75°. For every incident angle, 6 different reflectance curves are obtained by changing rotational angles of turntable from 0 to 360° at intervals of 60°, demonstrating the variation trends of reflectance peaks at different rotation angles for every incident angle.

they turn into dark brown as the whole wing patch tardily being soaked into the EtOH. Finally, they recover to initial vivid green color after drying in the air for a few seconds (Figure S4). Because pigments can usually be easily resolved into general organic solvents, for example, EtOH in this case, it indicates that the green color is attributed to structural color rather than pigment. In other words, the macroscopic vivid green color originates from the interactions between light and MHSs of butterfly wing scales. It further confirms that the original wing scales can manipulate visible light with their ultrafine MHSs.

To fully explore the relationships between optical properties of and orientations, omnidirectional reflective performance of the original wing scales is characterized in the round using a self-built spherical color observation system (SCOS, Figure S5). First, the reflective performance of the original wing scales is investigated in 2D plane. When the semiautomatic turntable rotated around the *z*-axis within 360°, the color images of the selected region are captured at the interval of 30° (Figure 2). Then RGB values of the specific site in the selected region are quantized using a color picker. With the semiautomatic turntable rotating from 0 to 180°, the selected region first changes from dark cyan to quartz color, then from 180 to 360°, it gradually recovers to dark cyan (Movie S2). The color changes are repeated in period of 180°. Two specific sites are of similar RGB values when the difference between their rotation angles is approximately one cycle (180°). RGB values at 0 versus 180°, and 90 versus 270° indicate colors changed slightly in the symmetrical observation point. According to the measurements, it seems that color intensities change slightly as hind wing rotating on $x-o-y$ plane, but color type almost maintains itself as initial state (green). It indicates that the vivid green color possesses reflective stability on 2D plane.

Omnidirectional Reflective Performance of Butterfly Wings. Considering it is impossible that a butterfly can always keep its wings level on a 2D plane in real situations, we hypothesize that the reflective stability of original wing scales can retain when extending dimensionality from 2D to 3D, which means omnidirectional stability in spatial domain. We then design an ingenious optical experiment to confirm the ORS properties of the original butterfly wing scales. Different with the case that reflectance changing at a fixed incident angle as turntable rotating, in this case, incident angles also change regularly leading to an omnidirectional view in 3D space.

A series of experimental reflectance spectra are achieved by changing incident angle of light from 0 to 75° at the interval of 15° and changing rotation angle of the turntable from 0 to 300° at the interval of 60° (Figure 3a–f, left). Interestingly, no matter how to change the incident angles of light and rotation angles of the turntable, these reflectance spectra almost demonstrate the similar unimodal tendency and the feature peaks always appear over green color waveband. Through fully comparative analysis, it is found that the feature peak intensities of reflectance spectra significantly change from the lowest 1.8% to highest 47.5%. Peak reflectance of the original wing scale with variable incident angles and rotation angles are also obtained (Figure 3a–f, right). With rotation angle changing

DOI: 10.1021/acsami.7b08768
ACS Appl. Mater. Interfaces 2017, 9, 29285–29294

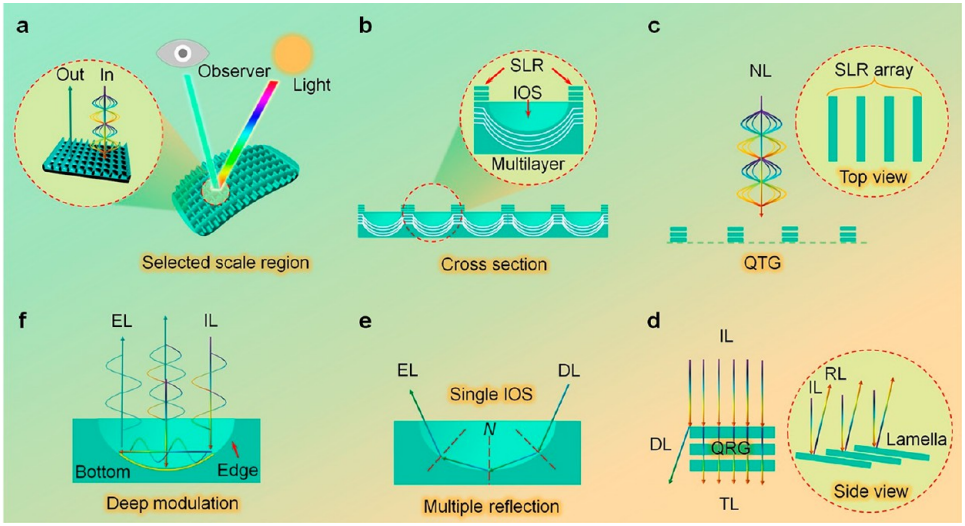

Figure 4. (a) Selected scale region of an original wing scale can turn incident multiwavelength light to special wavelength light received by observer, which acts as a light filter leading to a highly color selective. (b) Cross-section of the selected scale region demonstrates its basic structural components: periodic SLRs and multilayer IOSs (inset). (c) The natural light (NL) shines the SLR array that works as a QTG from the top view. (d) Overlapped lamellae as the QRG can manipulate the incident light (IL) and divided them into reflected light (RL) on the lamella surface, transmission light (TL) in the multilayer and diffraction light (DL) beside the SLRs. (e) When DL from the nearby SLR accesses into the single IOS, multiple reflection occurs on the inner surface of the IOS. (f) For normal IL, deep modulation effect can also occur on the inner surface of the IOS, leading to a special exit light (EL), which can significantly modulate the multiwavelength IL into the special EL.

from 0 to 300°, the reflectance intensity changes obviously, but the reflectance peaks shift slightly at the range of 520−550 nm, belonging to a typical green waveband (495−570 nm). The feature peak positions almost keep stable near 526 nm, which keeps consistent with the reflectance spectrum of the original wing scales at an initial angle (normal incidence). Thus, it is proved that original wing scales can firmly keep ORS properties no matter how the incident and rotational angles change in 3D space. On the basis of the previous relative researches,[4,50] it is speculated that the novel ORS properties may also arise from the optical interaction of light and structured surfaces of butterfly wings.

Mechanism Analysis of the ORS Properties. We figure it that natural MHSs may be responsible for the ORS properties of the butterfly wings. In order to fully reveal the underlying formation mechanism of the ORS properties, the physical interactions between light and the single scale with structure complex of SLR array and IOS array are schematically illustrated. For multiwavelength natural light incidence, the selected region of original wing scales shows highly selective reflection so that the natural green structural colors are observed directly (Figure 4a). In fact, the natural MHSs in butterfly wing scales can be divided into two important basic optical components: IOS and SLR. Thus, the selected scale region is a combination of multilayer IOSs and periodic SLRs. The cross-section of the selected scale region shows the spatial position relationship between IOS and SLR (Figure 4b).

On one hand, multiwavelength incident light will first cross the raised ridges before reaching the bottom and the edge of the IOS. From top view, it is interesting to find that these periodic SLRs form a ridge array that actually constitutes a quasi-transmission grating (QTG). The SLR array works as a multislit diffraction screen (Figure 4c). More interestingly, the overlapped lamellae of the single ridge form a quasi-reflection grating (QRG) from a side view (Figure 4d). As we know, both QTG and QRG can change the amplitudes of incident light and reflection light. Thus, they are so-called "amplitude grating", a kind of diffraction grating. In fact, the multislit diffraction grating is based on Fraunhofer diffraction effect to work. The relationship among grating structure, diffraction angle (θ) and incident light can be quantitatively described via eq 1 as follows:

$$d\sin\theta = n\lambda, \quad d = a + b \tag{1}$$

where d is grating constant representing the spacing between two adjacent slits, a is the width of the slit, b is the width of lighttight shield, n is diffraction series that could be any positive integer, and λ is the wavelength of incident light. Usually, d is at the nanoscale. However, the spacing between two adjacent ridges is about 8.36 μm, which is much broader than d. This can effectively avoid the possibility of surface diffraction to some extent. Most the incident light is reflected by the lamella surfaces, some crosses the alternating chitin-air layers, and others beside the ridge is diffracted by the QTG and gets into the nearby pits. Generally speaking, when the wavelength of incident light is close to the width of light-tight shield ($\lambda \rightarrow b$), the incident light can be more easily diffracted by the QTG. Then the diffracting light occurs multireflection on the pit surfaces before it escapes the pit as exiting light (Figure 4e). On the other hand, most natural light across the QTG reaches the inner surface (bottom and edge) of the IOS. Normal natural light shining onto the bowl bottom is directly reflected, while incident light shining onto the IOS edge occurs double reflection (Figure 4f). It is confirmed that the double reflection inside the pit will cause a polarization rotation when polarized light is imposed on the IOS surface. The main reason is that the polarized light is geometrically rotated by the plane reflections at the interface. Therefore, the ORS properties of original wing scales can be attributed to these integrated optical effects. It is also inferred that the MHSs lay the foundation for the novel ORS properties physically.

DOI: 10.1021/acsami.7b08768
ACS Appl. Mater. Interfaces 2017, 9, 29285−29294

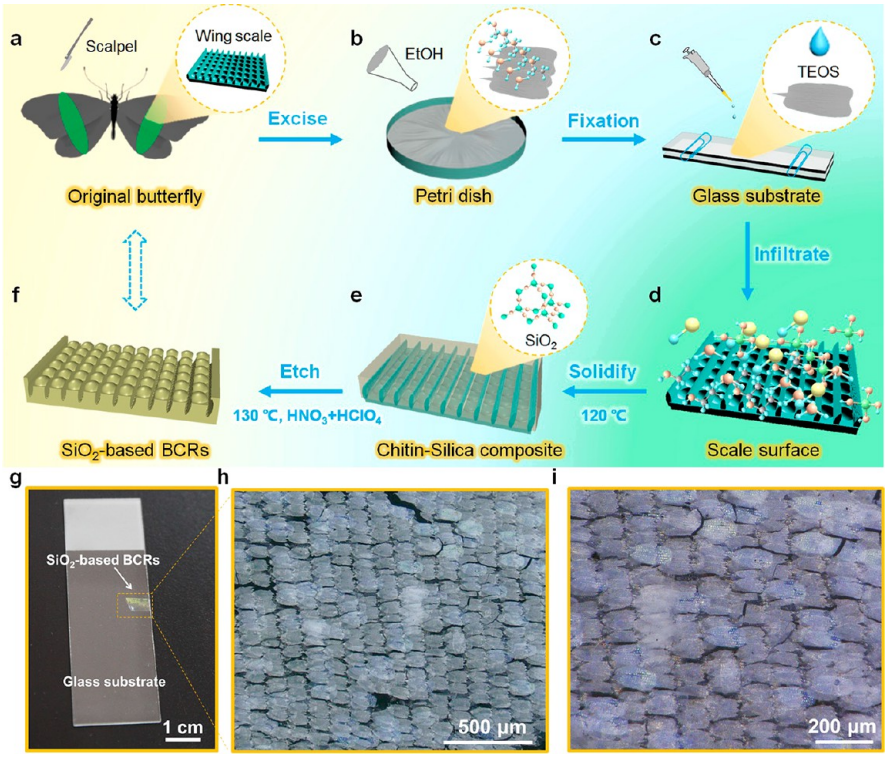

Figure 5. (a) Wing slice as a biotemplate was excised from original butterfly. (b) Biotemplate was totally soaked into organic solvent. (c) Precursor solution (TEOS) was injected into the gap of two glass substrate where the biotemplate was properly fixed. (d) Sol−gel reaction occurs in the original scale surface with MHSs. (e) SiO_2-based film generating along the MHSs of the biotemplate after solidification at 120 °C. (f) SiO_2-based BCRs were obtained after removing the biotemplate by etching. (g) Digital photo of the SiO_2-based BCRs with brilliant structural colors. (h, i) Stereoscopic microscope images of the BCRs resembling overlapped tiles on a roof under low and medium magnifications.

Bioinspired Design and Biomimetic Fabrication of SiO_2-Based Color Reflectors. As we know, a lot of organisms in nature are chitin-based, such as fungi, yeast, arthropods, cephalopods, mollusks, and insects.[17,51,52] Because chitin is a natural polysaccharide that is formed into well-organized structures, it is inferred that the original wing scales with ultrafine MHSs are also composed of chitin, a polymer of N-acetylglucosamine. Then the chemical elements of the specimen are characterized using an energy dispersive spectrometer (EDS). The EDS spectrum indicates the elemental composition of the original wing scales (Figure S6). There are three strong feature peaks appearing over a range of 0−2.5 keV. The result confirms the presence of the elements carbon (C), oxygen (O), and nitrogen (N), which is consistent with the frame elements of the chitin. The quantitative analysis further indicates C, O, and N are the main three chemical elements, the proportions (wt, %) of which are 58.46, 14.45, and 20.68 respectively (Table S1). The chemical compositions of original wing scales lay foundation for the following bioinspired design and biomimetic fabrication on a glass substrate via a facile biotemplate method under mild conditions (see Experimental Section).

The involved biomimetic fabrication method is facile and effective at low cost, combining a timesaving sol−gel technique and a selective etching process. Simplified 3D structural models are built to illustrate the key steps of the fabrication process of the SiO_2-based BCRs. Considering conventional machining accuracy is insufficient to fabricate such natural multiscale hierarchical structures, it inspired us to select the original wing scales as the initial biotemplate (Figure 5a). In order to enhance the mechanical strength of the biotemplate as well as remove the possible impurity filled in the micro/nanostructures, organic solvents (EtOH or diethyl ether) are used to soak the selected wing slice for a few minutes (Figure 5b). After the selected wing slice is drying in the air, we use the precursor solution, a mixture solution of tetraethylorthosilicate (TEOS) and EtOH with excellent liquidity, to immerse and fill the MHSs of the biotemplate (Figure 5c). Sol reaction occurs on the scale surface (Figure 5d). Then the biotemplate is heated to make the sol filled in the MHSs gradually solidified to form the SiO_2-based 3D networks (Figure 5e). In fact, the SiO_2-based 3D networks play a vital role in the framework formation of the BCRs. It involves a two-step hydrolytic polymerization reaction of TEOS in the precursor solution. The formation mechanism of the SiO_2-based 3D networks is briefly illustrated (Figure S7). Step one, hydrolysis reaction of TEOS occurs under acidic conditions or at low pH environment to generate hydrated silica $[(EtO)_2Si(OH)_2]$ and EtOH. Meanwhile, condensation reaction of TEOS and $(EtO)_2Si(OH)_2$ occurs to form the colloid mixture, a transparent and homogeneous suspensions. Step two, condensation reaction between $(EtO)_2Si(OH)_2$ and SiO_2 clusters occurs and cross-linked SiO_2 cluster and H_2O are generated. The aforementioned chemical reactions constitute the main body of the sol−gel process. Finally, these cross-linked SiO_2 clusters further linked together to form the SiO_2-based 3D networks via the polymerization reaction of oligomers. After removing the biotemplate, the SiO_2-based BCRs with complex structures were obtained (Figure 5f).

The BCRs on a glass substrate demonstrate brilliant structural colors (Figure 5g). It indicates the BCRs are structure-based at macro level. Meanwhile, the dynamic photos of the BCRs on a glass substrate were also obtained at the

DOI: 10.1021/acsami.7b08768
ACS Appl. Mater. Interfaces 2017, 9, 29285−29294

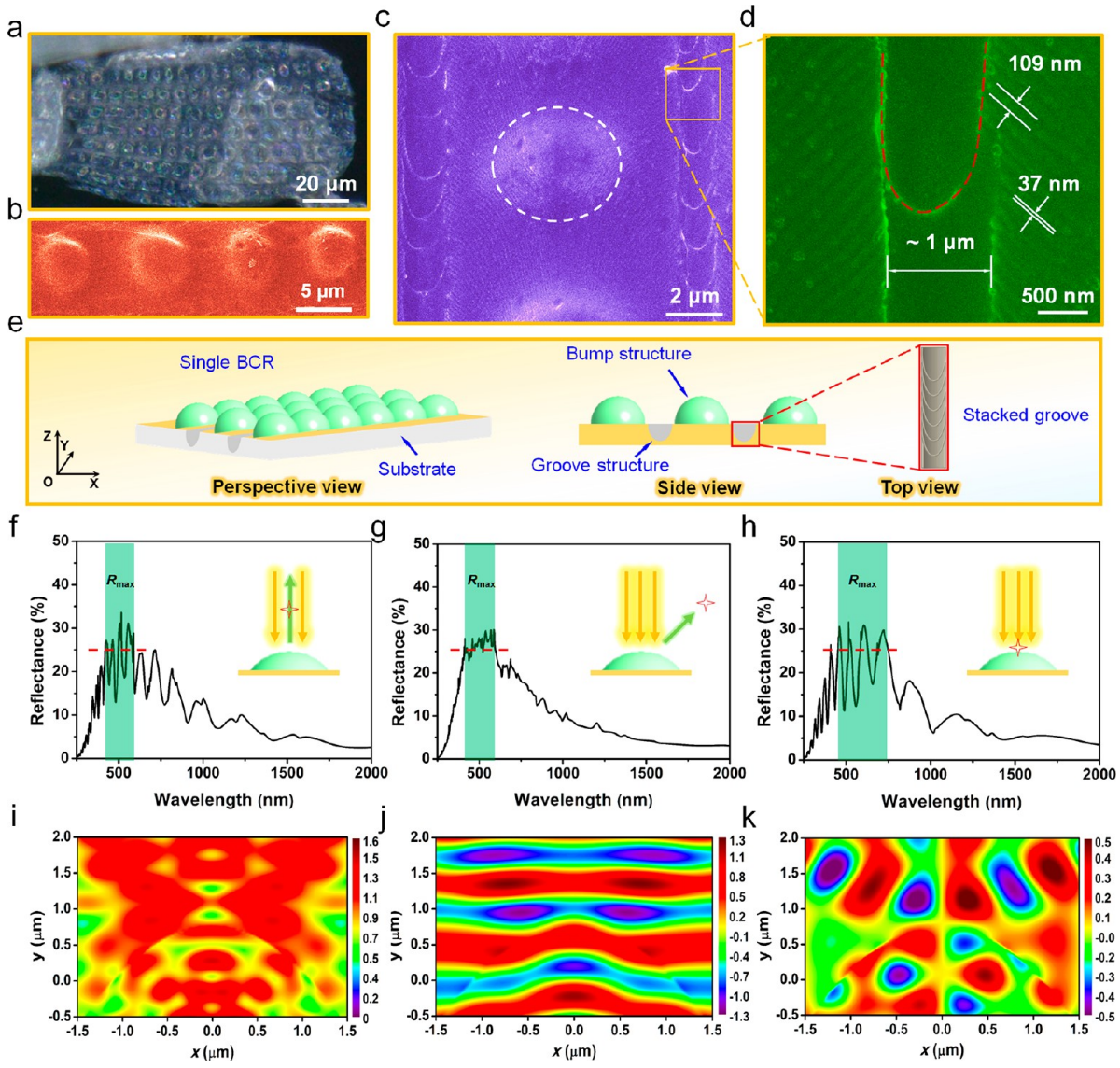

Figure 6. (a) Single biomimetic BCR with artificial structures also showing brilliant structural colors. (b) Highly ordered bump structure array. (c) Individual bump structure with oval shape. (d) Groove structure with regular textures besides the bump. (e) Schematic illustration of two typical periodic structures in the BCR: bump structure and groove structure. Simulated reflectance of special monitoring sites near a single bump structure of the SiO_2-based BCR: (f) paralleling to the incident light (0°), (g) making 45° with the incident light, and (h) at the bump surface. (i) Electric field (E) profile at the $z = 0$ plane for the bump structure when plane wave light was injected from top to bottom. (j) X-component of the electric field (E_x). (k) Y-component of the electric field (E_y).

interval of 30° within 360° (Figure S8). Although the reflectance intensity of the BCRs is not as strong as that of original biotemplate, the SiO_2-based BCRs demonstrate relatively stable light green structural colors over a whole rotation period. It suggests that the obtained BCRs possess the similar ORS properties with the original biotemplate. According to a notable view structure determines function, it infers that the SiO_2-based BCRs might also be multiscale and hierarchical. Then morphologies and dimensions of the SiO_2-based BCRs were characterized. It is clear that the squamose BCRs arrange in good order (Figure 5h). The structural integrity of every single BCR is preserved completely. It is easy to understand that the BCRs inherit the squamose shapes from the original wing scales. With the magnification increasing, the structural morphology of the BCRs is observed clearly (Figure 5i). The BCRs are composed of abundant neatly arranged biomimetic scales. Interestingly, all these SiO_2-based biomimetic scales also exhibit brilliant structural colors at micro level. It suggests the SiO_2-based BCRs possess MHSs to a great extent.

Optical Performance of the BCRs. In order to further characterize the MHSs of the SiO_2-based BCRs, a single BCR with scale shape is enlarged for observation. It is noted that there are a large number of bump structures resembling smooth colorful soap bubbles on the BCR surface (Figure 6a). These bump structures regularly arrange in array (Figure 6b). In fact, there are serried textures on the surface of every single bump, which originates from the fine hierarchical structures inside the original pits. In addition, groove structures with folded textures are laid on both side of the bump structure (Figure 6c). Beside the main groove structure, microgrooves are parallel and at about 45° with the main groove (Figure 6d). To further understand the overall morphology of the BCRs, we built 3D visual models to briefly illustrate the feature structures in a single BCR from three different views (Figure 6e). It was easy

DOI: 10.1021/acsami.7b08768
ACS Appl. Mater. Interfaces 2017, 9, 29285−29294

to understand that the feature structures arise from the original MHSs filled with the nanoscale SiO_2 during the biomimetic fabrication process. In fact, the bump structures and groove structures on the glass substrate together constitute the main body of the SiO_2-based BCRs.

Optical performance of the SiO_2-based BCRs is characterized using the finite difference time domain (FDTD) method. FDTD method is good at solving optical issues and has the capability to simulate and analyze light interactions with the structured surfaces.[47] Because the BCRs are mainly composed of periodic and symmetric structure units, a simplified optical model of the BCRs was applied to the local reflectance simulations using FDTD method. Moreover, the visible structural colors are directly presented by the bump structure rather than groove structure. Naturally, bump structure was selected as the simulation object in this case (Figure S9). The simulated reflectance as a function of the wavelength at three different positions was then obtained (Figure 6f−h). The simulated maximal reflectance values of the BCRs are all about 30% near 520 nm, which are in good accordance with experimental reflectance of the original biotemplate. Meanwhile, electric field profiles at selected wavelengths can also provide additional insight into the optical interaction between incident light (350−1000 nm) and the MHSs.[53] Because bump structure is the first obstacle that incident light will encounter, the relative contribution of the bump structure to light reflection is very essential for understanding the ORS properties of the BCRs. FDTD results indicate the intensive electric field enhancement occurs around the bump surface (Figure 6i). It suggests that this optimal structure demonstrates strong reflectance in a wide space. Dynamic electric field changes also demonstrate significant light−matter effect occurs near the bump structure after incident light is injected at normal (Movie S3). Particularly, obvious warps of electric field can be observed when incident light draw close to the bump structure (Figure 6j). Moreover, the intensity of electric field presents excellent space symmetry due to the symmetry of the bump structure (Figure 6k). According to the comparison of the experimental and simulated results on both morphology characterizations (Chart S1) and optical performances, it confirms that both the graceful MHSs and novel ORS properties of the natural biotemplate have been well-inherited by the SiO_2-based BCRs.

CONCLUSION

In summary, we experimentally demonstrate and theoretically investigate the MHS-based ORS properties of *Papilio palinurus* butterfly wing scales. Biological morphologies of the original wing scales with MHSs are characterized in detail at multiscale levels. Our dynamic optical spectrum analysis shows the ORS properties are caused by the integrated optical effects between light and the MHSs. Inspired by the novel ORS properties in butterfly wing scales, SiO_2-based BCRs are mimicked successfully on a glass substrate using a biotemplate method. The involved biomimetic fabrication method is facile and effective at low cost, combining the sol−gel technique and a selective etching process. Interestingly, the biomimetic BCRs not only demonstrate similar structural colors with original biotemplate but also inherit its ORS properties. The morphology and dimension comparisons between original biotemplate and SiO_2-based BCRs indicate the natural MHSs are effectively inherited with high uniformity and fidelity. It is convincingly confirmed by the experimental results that the proposed biotemplate method is well suitable to replicate natural MHSs.

We anticipated that the SiO_2-based BCRs inspired by butterfly wing scales could provide a promising strategy to mimic complex structured surfaces with ultrafine MHSs and probably and bridge the gap between novel bioinspired materials and potential practical applications in many optical devices, displays, and other optoelectronic equipment.

EXPERIMENTAL SECTION

Original Wing Scales. The pretreatment vivid green scale region of *Papilio palinurus* butterfly hind wing is used as experimental materials to do further research.

Discoloration Experiment. A simple discoloration experiment is carried out to confirm that the brilliant colors of the wing scales are mainly structure-based rather than pigment. First, the neat and clean green scale region is cut off the right hind wing meticulously using a scalpel in perpendicular and parallel directions to the nervure, respectively. Then, the specimen is clamped with a tweezer to flatwise place in a Petri dish. In order to degrease the wing tissue and increase its mechanical strength, the specimen is soaked into a certain amount of diethyl ether (A. R.) and absolute ethanol (A. R.) for 10 min, respectively. The colors of the specimen are still brilliant after natural drying, which are not affected by the organic solvents virtually. Diethyl ether (A. R.) and EtOH (A. R.) are provided by Tianjin Fuyu Fine Chemical Co., Ltd.

Morphology and Dimension Characterization. With the help of 3D ultradepth stereoscopic microscope (KEYENCE VHX-5000) and ultrahigh-resolution FESEM (ZEISS MERLIN Compact), the morphologies and dimension of both the original wing scales and the biomimetic replicas are characterized under different magnifications. With the magnification increasing, more details are observed clearly.

3D Optimized Visual Structure Models. According to the FESEM images, a series of optimized visual 3D models of the multiscale structures in original wing scales and the BCRs on glass substrate were built. These simplified 3D models were used to briefly illustrate the structure morphologies of original wing scales and the biomimetic fabrication process.

Spectrum Characterization. The reflectance spectra of the original wing scales and the biomimetic replicas over a range of 450−950 nm wavelengths is obtained using a miniature fiber-optic spectrometer (Ocean Optics USB 4000). The spectrometer is carefully calibrated with STD-WS, a standard white board certified by the National Institute of Metrology of China.

Chemical Component Analysis and Element Distribution Characterization. An EDS (OXFORD X-Max^N 150) is applied to analysis the chemical components and characterize the element distributions of the chitin-based original wing scales.

Biomimetic Fabrication of SiO_2-Based BCRs. A kind of two-step and in situ biotemplate method combining the sol−gel technique and a selective etching process is adopted to fabricate the SiO_2-based BCRs. First of all, a slice of the pretreated butterfly wing (1 cm × 2 cm) is sandwiched between two clean glass slides. Both ends of the glass slides are clamped by clips with a proper force. Then, a certain amount of precursor solution (~10 μL) is added to the edge of the assembly with a micropipette, which is a compound of TEOS and hydrochloric acid (~3:1 in volume). Because of the capillary action between two glass slides, the precursor solution infiltrate into the micro/nanostructures of the wing scales spontaneously. To evaporate the residual precursor solution, the entire assembly is heated at 120 °C for 30 min in a drying oven, leading to the expected SiO_2 solidification in the wing scales. Subsequently, the clips are picked down with a tweezer carefully to avoid destroying the crisp SiO_2 multiscale structures. After that, the assembly is wholly dipped into a mixture of the concentrated nitric acid (A. R.) and perchloric acid (A. R.) (1:1 in volume). After heat treatment at 130 °C for another 30 min, the biotemplate is removed completely due to the corrosive effect of the mixed acids. Finally, the BCRs are obtained after washed by ultrasonic oscillation for 10 min with deionized water. The fabricated biomimetic

DOI: 10.1021/acsami.7b08768
ACS Appl. Mater. Interfaces 2017, 9, 29285−29294

replicas are well-preserved in a slide box. Concentrated nitric acid (A. R.) and TEOS are provided by Beijing Chemical Works, and perchloric acid and hydrochloric acid are provided by Changchun Hongyu Chemical Co., Ltd.

FDTD Simulations. In this case, the BCRs are composed of similar structure units. Notably, these structure units are not only periodic but also symmetric, which allows us to adopt 2D simulation region to simulate the reflection effect of the biomimetic bump structure. In addition, 2D simulation region is also a time-saving but effective choice to intensively study the optical performance in a reasonable simulation time. In consideration of the periodic structures along every individual scale, given boundary conditions of x and y are periodic and PML, respectively. Mesh type is autouniform and mesh accuracy is 2. The light source is plane wave with selected wavelengths of 350−1000 nm. Other parameters are set as default.

■ ASSOCIATED CONTENT

Supporting Information

The Supporting Information is available free of charge on the ACS Publications website at DOI: 10.1021/acsami.7b08768.

More details about the experimental and simulation methods; supplemental results of material morphology characterization and chemical elemental analysis; self-built spherical color observation system; sol−gel reaction mechanism and FDTD simulations (PDF)

Movie S1, dynamic color changes of the selected original wing slice in the discoloration process (AVI)

Movie S2, dynamic color changes of selected green region on hind wing surface with rotation angle changing at the rotation interval of 15° each time (AVI)

Movie S3, plane wave with selected wavelengths 350−1000 nm irradiation on the optical model (AVI)

■ AUTHOR INFORMATION

Corresponding Author

*E-mail: niushichao@jlu.edu.cn.

ORCID

Zhengzhi Mu: 0000-0001-9200-5498

Shichao Niu: 0000-0003-0208-9996

Author Contributions

‖Z.M., S.N., and Z.H. designed the experiments. Z. M., B.L.X.F., and Z.W. performed the experiments. J. Z. and S. N. helped with data analysis and theoretical simulation. Z. M., S. N. and Z. H. proposed the mechanism of ORS properties. Z. M., S. N., and Z. H. contributed to the writing of the manuscript. Z.H. and L.R. conceived the project. Z.H. and Z.M. contributed equally to this work.

Notes

The authors declare no competing financial interest.

■ ACKNOWLEDGMENTS

This work was supported by the National Natural Science Foundation of China (51325501, 51505183, and 51290292), China Postdoctoral Science Foundation Funded Project (2015M571360), Joint Construction Project of Jilin University and Jilin Province (SF2017-3-4), Outstanding Young Talent Fund of Jilin Province (20170520095JH), Chinese Government Scholarship from China Scholarship Council (201606170205), and Graduate Innovation Fund of Jilin University (2016020).

■ REFERENCES

(1) Vukusic, P.; Sambles, J.; Lawrence, C. Structural Colour: Colour Mixing in Wing Scales of a Butterfly. *Nature* **2000**, *404*, 457−457.

(2) Vukusic, P.; Sambles, J.; Lawrence, C.; Wootton, R. Structural Colour: Now You See It—Now You Don't. *Nature* **2001**, *410*, 36−36.

(3) Graham-Rowe, D. Tunable Structural Colour. *Nat. Photonics* **2009**, *3*, 551.

(4) Kolle, M.; Salgard-Cunha, P. M.; Scherer, M. R.; Huang, F.; Vukusic, P.; Mahajan, S.; Baumberg, J. J.; Steiner, U. Mimicking the Colourful Wing Scale Structure of the *Papilio Blumei* Butterfly. *Nat. Nanotechnol.* **2010**, *5*, 511−5.

(5) Song, B.; Johansen, V. E.; Sigmund, O.; Shin, J. H. Reproducing the Hierarchy of Disorder for *Morpho*-Inspired, Broad-Angle Color Reflection. *Sci. Rep.* **2017**, *7*, 46023.

(6) Chen, H.; Zhang, P.; Zhang, L.; Liu, H.; Jiang, Y.; Zhang, D.; Han, Z.; Jiang, L. Continuous Directional Water Transport on the Peristome Surface of *Nepenthes Alata*. *Nature* **2016**, *532*, 85−89.

(7) Clapham, P.; Hutley, M. Reduction of Lens Reflexion by the "Moth Eye" Principle. *Nature* **1973**, *244*, 281.

(8) Mokarian-Tabari, P.; Senthamaraikannan, R.; Glynn, C.; Collins, T. W.; Cummins, C.; Nugent, D.; O'Dwyer, C.; Morris, M. A. Large Block Copolymer Self-Assembly for Fabrication of Subwavelength Nanostructures for Applications in Optics. *Nano Lett.* **2017**, *17*, 2973.

(9) Barthlott, W.; Neinhuis, C. Purity of the Sacred Lotus, or Escape from Contamination in Biological Surfaces. *Planta* **1997**, *202*, 1−8.

(10) Ju, J.; Bai, H.; Zheng, Y.; Zhao, T.; Fang, R.; Jiang, L. A Multi-Structural and Multi-Functional Integrated Fog Collection System in Cactus. *Nat. Commun.* **2012**, *3*, 1247.

(11) Li, K.; Ju, J.; Xue, Z.; Ma, J.; Feng, L.; Gao, S.; Jiang, L. Structured Cone Arrays for Continuous and Effective Collection of Micron-Sized Oil Droplets from Water. *Nat. Commun.* **2013**, *4*, 2276.

(12) Gao, X.; Jiang, L. Biophysics: Water-Repellent Legs of Water Striders. *Nature* **2004**, *432*, 36.

(13) England, G.; Kolle, M.; Kim, P.; Khan, M.; Munoz, P.; Mazur, E.; Aizenberg, J. Bioinspired Micrograting Arrays Mimicking the Reverse Color Diffraction Elements Evolved by the Butterfly *Pierella Luna*. *Proc. Natl. Acad. Sci. U. S. A.* **2014**, *111*, 15630−4.

(14) Werner, T.; Koshikawa, S.; Williams, T. M.; Carroll, S. B. Generation of a Novel Wing Colour Pattern by the Wingless Morphogen. *Nature* **2010**, *464*, 1143−8.

(15) Li, L.; Kolle, S.; Weaver, J. C.; Ortiz, C.; Aizenberg, J.; Kolle, M. A Highly Conspicuous Mineralized Composite Photonic Architecture in the Translucent Shell of the Blue-Rayed Limpet. *Nat. Commun.* **2015**, *6*, 6322.

(16) Xiao, M.; Li, Y.; Allen, M. C.; Deheyn, D. D.; Yue, X.; Zhao, J.; Gianneschi, N. C.; Shawkey, M. D.; Dhinojwala, A. Bio-Inspired Structural Colors Produced *via* Self-Assembly of Synthetic Melanin Nanoparticles. *ACS Nano* **2015**, *9*, 5454−5460.

(17) Parker, A. R.; Townley, H. E. Biomimetics of Photonic Nanostructures. *Nat. Nanotechnol.* **2007**, *2*, 347−353.

(18) Yu, K.; Fan, T.; Lou, S.; Zhang, D. Biomimetic Optical Materials: Integration of Nature's Design for Manipulation of Light. *Prog. Mater. Sci.* **2013**, *58*, 825−873.

(19) Zheng, X.; Shen, G.; Wang, C.; Li, Y.; Dunphy, D.; Hasan, T.; Brinker, C. J.; Su, B. L. Bio-Inspired Murray Materials for Mass Transfer and Activity. *Nat. Commun.* **2017**, *8*, 14921.

(20) Wang, W.; Zhang, W.; Fang, X.; Huang, Y.; Liu, Q.; Gu, J.; Zhang, D. Demonstration of Higher Colour Response with Ambient Refractive Index in *Papilio Blumei* as Compared to *Morpho Rhetenor*. *Sci. Rep.* **2015**, *4*, 5591.

(21) Huang, J.; Wang, X.; Wang, Z. L. Controlled Replication of Butterfly Wings for Achieving Tunable Photonic Properties. *Nano Lett.* **2006**, *6*, 2325−2331.

(22) Kim, H.; Lee, H.-B.-R.; Maeng, W. J. Applications of Atomic Layer Deposition to Nanofabrication and Emerging Nanodevices. *Thin Solid Films* **2009**, *517*, 2563−2580.

(23) Liu, F.; Liu, Y.; Huang, L.; Hu, X.; Dong, B.; Shi, W.; Xie, Y.; Ye, X. Replication of Homologous Optical and Hydrophobic Features by

Templating Wings of Butterflies *Morpho Menelaus*. *Opt. Commun.* **2011**, *284*, 2376−2381.
(24) Kanamori, Y.; Roy, E.; Chen, Y. Antireflection Sub-Wavelength Gratings Fabricated by Spin-Coating Replication. *Microelectron. Eng.* **2005**, *78*, 287−293.
(25) Han, K.-S.; Shin, J.-H.; Lee, H. Enhanced Transmittance of Glass Plates for Solar Cells Using Nano-Imprint Lithography. *Sol. Energy Mater. Sol. Cells* **2010**, *94*, 583−587.
(26) Song, Y. M.; Bae, S. Y.; Yu, J. S.; Lee, Y. T. Closely Packed and Aspect-Ratio-Controlled Antireflection Subwavelength Gratings on Gaas Using a Lenslike Shape Transfer. *Opt. Lett.* **2009**, *34*, 1702−1704.
(27) Sai, H.; Fujii, H.; Arafune, K.; Ohshita, Y.; Yamaguchi, M.; Kanamori, Y.; Yugami, H. Antireflective Subwavelength Structures on Crystalline Si Fabricated Using Directly Formed Anodic Porous Alumina Masks. *Appl. Phys. Lett.* **2006**, *88*, 201116.
(28) Kanamori, Y.; Hane, K.; Sai, H.; Yugami, H. 100 Nm Period Silicon Antireflection Structures Fabricated Using a Porous Alumina Membrane Mask. *Appl. Phys. Lett.* **2001**, *78*, 142−143.
(29) Min, W.-L.; Betancourt, A. P.; Jiang, P.; Jiang, B. Bioinspired Broadband Antireflection Coatings on Gasb. *Appl. Phys. Lett.* **2008**, *92*, 141109.
(30) Zhang, F.; Shen, Q.; Shi, X.; Li, S.; Wang, W.; Luo, Z.; He, G.; Zhang, P.; Tao, P.; Song, C.; et al. Infrared Detection Based on Localized Modification of *Morpho* Butterfly Wings. *Adv. Mater.* **2015**, *27*, 1077−1082.
(31) Zhang, D.; Zhang, W.; Gu, J.; Fan, T.; Liu, Q.; Su, H.; Zhu, S. Inspiration from Butterfly and Moth Wing Scales: Characterization, Modeling, and Fabrication. *Prog. Mater. Sci.* **2015**, *68*, 67−96.
(32) Watanabe, K.; Hoshino, T.; Kanda, K.; Haruyama, Y.; Matsui, S. Brilliant Blue Observation from a *Morpho*-Butterfly-Scale Quasi-Structure. *Jpn. J. Appl. Phys.* **2005**, *44*, L48−L50.
(33) Wang, X.; Liao, Y.; Liu, B.; Ge, L.; Li, G.; Fu, S.; Chen, Y.; Cui, Z. Free-Standing SU-8 Subwavelength Gratings Fabricated by UV Curing Imprint. *Microelectron. Eng.* **2008**, *85*, 910−913.
(34) Chen, H.; Chuang, S.; Lin, C.; Lin, Y. Using Colloidal Lithography to Fabricate and Optimize Sub-Wavelength Pyramidal and Honeycomb Structures in Solar Cells. *Opt. Express* **2007**, *15*, 14793−14803.
(35) Li, Y.; Zhang, J.; Zhu, S.; Dong, H.; Jia, F.; Wang, Z.; Sun, Z.; Zhang, L.; Li, Y.; Li, H.; et al. Biomimetic Surfaces for High-Performance Optics. *Adv. Mater.* **2009**, *21*, 4731−4734.
(36) Hung, Y., Jr; Lee, S.-L.; Coldren, L. A. Deep and Tapered Silicon Photonic Crystals for Achieving Anti-Reflection and Enhanced Absorption. *Opt. Express* **2010**, *18*, 6841−6852.
(37) Lohmüller, T.; Helgert, M.; Sundermann, M.; Brunner, R.; Spatz, J. P. Biomimetic Interfaces for High-Performance Optics in the Deep-UV Light Range. *Nano Lett.* **2008**, *8*, 1429−1433.
(38) Zhao, Y.; Xie, Z.; Gu, H.; Zhu, C.; Gu, Z. Bio-Inspired Variable Structural Color Materials. *Chem. Soc. Rev.* **2012**, *41*, 3297−317.
(39) Braun, P. V. Materials Science: Colour without Colourants. *Nature* **2011**, *472*, 423−424.
(40) Kim, H.; Ge, J.; Kim, J.; Choi, S.-e.; Lee, H.; Lee, H.; Park, W.; Yin, Y.; Kwon, S. Structural Colour Printing Using a Magnetically Tunable and Lithographically Fixable Photonic Crystal. *Nat. Photonics* **2009**, *3*, 534−540.
(41) Kolle, M.; Lethbridge, A.; Kreysing, M.; Baumberg, J. J.; Aizenberg, J.; Vukusic, P. Bio-Inspired Band-Gap Tunable Elastic Optical Multilayer Fibers. *Adv. Mater.* **2013**, *25*, 2239−45.
(42) Aizenberg, J.; Sundar, V. C.; Yablon, A. D.; Weaver, J. C.; Chen, G. Biological Glass Fibers: Correlation between Optical and Structural Properties. *Proc. Natl. Acad. Sci. U. S. A.* **2004**, *101*, 3358−63.
(43) Lou, S.; Guo, X.; Fan, T.; Zhang, D. Butterflies: Inspiration for Solar Cells and Sunlight Water-Splitting Catalysts. *Energy Environ. Sci.* **2012**, *5*, 9195−9216.
(44) Zhao, Q.; Guo, X.; Fan, T.; Ding, J.; Zhang, D.; Guo, Q. Art of Blackness in Butterfly Wings as Natural Solar Collector. *Soft Matter* **2011**, *7*, 11433−11439.
(45) Han, Z. W.; Niu, S. C.; Li, W.; Ren, L. Q. Preparation of Bionic Nanostructures from Butterfly Wings and Their Low Reflectivity of Ultraviolet. *Appl. Phys. Lett.* **2013**, *102*, 233702.
(46) Han, Z.; Mu, Z.; Li, B.; Wang, Z.; Zhang, J.; Niu, S.; Ren, L. Active Antifogging Property of Monolayer SiO_2 Film with Bioinspired Multiscale Hierarchical Pagoda Structures. *ACS Nano* **2016**, *10*, 8591−8602.
(47) Butt, H.; Yetisen, A. K.; Mistry, D.; Khan, S. A.; Hassan, M. U.; Yun, S. H. *Morpho* Butterfly-Inspired Nanostructures. *Adv. Adv. Opt. Mater.* **2016**, *4*, 497−504.
(48) Pris, A. D.; Utturkar, Y.; Surman, C.; Morris, W. G.; Vert, A.; Zalyubovskiy, S.; Deng, T.; Ghiradella, H. T.; Potyrailo, R. A. Towards High-Speed Imaging of Infrared Photons with Bio-Inspired Nano-architectures. *Nat. Photonics* **2012**, *6*, 195−200.
(49) Zhou, L.; Dong, X.; Zhou, Y.; Su, W.; Chen, X.; Zhu, Y.; Shen, S. Multiscale Micro-Nano Nested Structures: Engineered Surface Morphology for Efficient Light Escaping in Organic Light-Emitting Diodes. *ACS Appl. Mater. Interfaces* **2015**, *7*, 26989−98.
(50) Diao, Y.-Y.; Liu, X.-Y. Mysterious Coloring: Structural Origin of Color Mixing for Two Breeds of *Papilio* Butterflies. *Opt. Express* **2011**, *19*, 9232−9241.
(51) Srinivasarao, M. Nano-Optics in the Biological World: Beetles, Butterflies, Birds, and Moths. *Chem. Rev.* **1999**, *99*, 1935−1962.
(52) Weatherspoon, M. R.; Cai, Y.; Crne, M.; Srinivasarao, M.; Sandhage, K. H. 3d Rutile Titania-Based Structures with *Morpho* Butterfly Wing Scale Morphologies. *Angew. Chem., Int. Ed.* **2008**, *47*, 7921−3.
(53) Feng, W.; Kim, J.-Y.; Wang, X.; Calcaterra, H. A.; Qu, Z.; Meshi, L.; Kotov, N. A. Assembly of Mesoscale Helices with near-Unity Enantiomeric Excess and Light-Matter Interactions for Chiral Semiconductors. *Sci. Adv.* **2017**, *3*, e1601159.

DOI: 10.1021/acsami.7b08768
ACS Appl. Mater. Interfaces 2017, 9, 29285−29294